

Unified approach to nuclear densities from exotic atoms

E. Friedman^{1,*}

¹*Racah Institute of Physics, The Hebrew University, Jerusalem 91904, Israel*

(Dated: November 5, 2018)

Parameters of nuclear density distributions are derived from least-squares fits to strong interaction observables in exotic atoms. Global analyses of antiprotonic and pionic atoms show reasonably good agreement between the two types of probes regarding the average behaviour of root-mean-square radii of the neutron distributions. Apparent conflict regarding the shape of the neutron distribution is attributed to different radial sensitivities of these two probes.

PACS numbers: 21.10.Gv, 25.43.+t, 25.80.Hp, 36.10.Gv

Keywords: Antiprotonic atoms, Pionic atoms, Neutron densities

I. INTRODUCTION

The density distribution of protons in nuclei is considered known as it is obtained from the nuclear charge distribution by unfolding the finite size of the charge of the proton. The neutron distributions are, however, generally not known to sufficient accuracy. A host of different methods has been applied in studies of root-mean-square (rms) radii of neutron distributions in nuclei but the results are sometimes conflicting, see e.g. [1, 2]. In the present work we focus on antiprotonic and on pionic atoms as a source of information on neutron densities. We deduce average properties with the help of global analyses of about 100 data points in each case, covering the whole of the periodic table. Reasonably good agreement is obtained between the two types of exotic atoms when considering rms radii of the neutron distributions. A conflict regarding the shape of the distributions is most likely due to the different radial sensitivities of the two probes.

II. METHOD

Strong interaction level shifts and widths in exotic atoms, formed by the capture of a negatively charged hadron into an atomic orbit, are calculated with the help of an optical potential inserted into the appropriate wave equation. The simplest class of optical potentials V_{opt} is the generic $t\rho(r)$ potential, which for underlying s -wave hadron-nucleon interactions assumes the form:

$$2\mu V_{\text{opt}}(r) = -4\pi\left(1 + \frac{A-1}{A} \frac{\mu}{M}\right)\{b_0[\rho_n(r) + \rho_p(r)] + \tau_z b_1[\rho_n(r) - \rho_p(r)]\}. \quad (1)$$

Here, ρ_n and ρ_p are the neutron and proton density distributions normalized to the number of neutrons N and number of protons Z , respectively, M is the mass of the nucleon and $\tau_z = +1$ for the negatively charged hadrons considered

*Electronic address: elifried@vms.huji.ac.il

in the present work. When handling many different nuclei over the periodic table it is necessary to represent the densities by approximate distributions, usually chosen as the two-parameter Fermi distribution (2pF). With the proton densities considered known, we focus on the differences between the neutron and the proton distributions. A linear dependence of $r_n - r_p$, the difference between the rms radii, on $(N - Z)/A$ has been employed in \bar{p} studies [2, 3, 4], namely

$$r_n - r_p = \gamma \frac{N - Z}{A} + \delta, \quad (2)$$

with γ close to 1.0 fm and δ close to zero. This parameterization is adopted here. In order to allow for possible differences in the shape of the neutron distribution, the ‘skin’ and ‘halo’ forms of Ref. [3] were used, as well as an average between the two. We adopt a 2pF distribution both for the proton (unfolded from the charge distribution) and for the neutron density distributions

$$\rho_{n,p}(r) = \frac{\rho_{0n,0p}}{1 + \exp((r - R_{n,p})/a_{n,p})}. \quad (3)$$

Then for each value of $r_n - r_p$ in the ‘skin’ form the same diffuseness parameter for protons and neutrons, $a_n = a_p$, is used and the R_n parameter is determined from the rms radius r_n . In the ‘halo’ form the same radius parameter, $R_n = R_p$, is assumed and a_n^h is determined from r_n . In the ‘average’ option the diffuseness parameter is set to be the average of the above two diffuseness parameters, $a_n^{\text{ave}} = (a_p + a_n^h)/2$, and the radius parameter R_n is then determined from the rms radius r_n . In this way we can test three shapes of the neutron distribution for each value of its rms radius all along the periodic table. These shapes provide sufficient difference in order to be tested in global fits. The results below are presented as the best fit χ^2 values *vs.* the neutron rms radius parameter γ .

III. RESULTS

A. Antiprotonic atoms

Figure 1 shows results of global fits to 90 data points from measurements of X-rays by the PS209 collaboration [5]. It is seen that the ‘skin’ shape for the neutron density distribution is unfavoured and that a finite range for the \bar{p} N interaction leads to significant improvements in the fits. Comparing the zero-range (ZR) results of the left-hand side of Fig.1 with the corresponding ZR results of Ref.[2] we note that the values of the best-fit parameter γ are quite different. This is due to the use in Ref.[2] of *fixed* values for the complex parameter b_0 for all values of γ whereas we re-fit these phenomenological parameters when γ changes. In fact, with the fixed values for b_0 taken from Ref.[6] one obtains a value for γ that merely represents an average over the neutron densities used in Ref.[6] to derive those fixed values.

The best fit finite-range potential produces a χ^2 per degree of freedom of about 2, which is most acceptable considering the simplicity of the model and the extent of the data. We also note that on the basis of values of χ^2 it is impossible to distinguish between the ‘halo’ and the ‘average’ shapes, which lead to somewhat different values of the rms radius parameter γ . Similar analyses of the radio-chemical data and of the combined X-rays and radiochemical data lead to very similar conclusions. It is interesting to note that the isovector parameter b_1 turns out to be consistent with zero [4]. This is in full agreement with the result of analysing separately the radio-chemical data where we find that the best fit is obtained for a ratio of 0.99 ± 0.07 for the absorption on a neutron to the absorption on a proton.

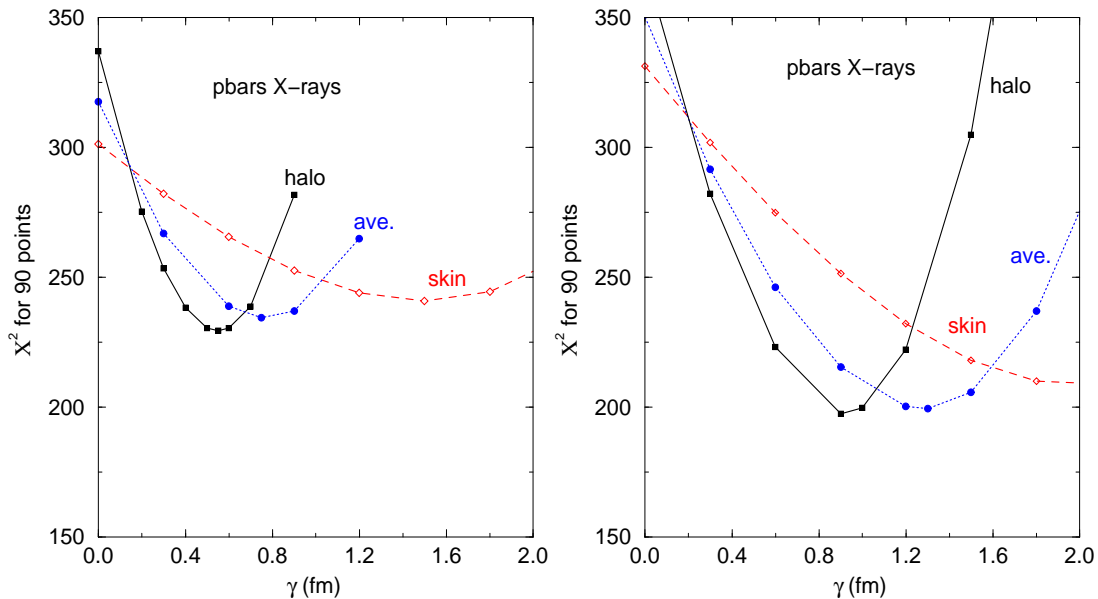


FIG. 1: Zero range (left) and finite range (right) fits to strong interaction shifts and widths in antiprotonic atoms. For the latter the best fit is obtained for a rms radius of the $\bar{p}N$ interaction of 1.1 ± 0.1 fm.

B. Pionic atoms

Values of rms radii of neutron distributions for several nuclides had been derived from pionic atoms more than two decades ago [1]. The first to derive rms radii from extensive data sets of strong interaction observables in pionic atoms were García-Recio et al. [7]. Using the ‘skin’ shape for the neutron densities they presented a list of rms radii which, when interpreted with the present formulation, leads to $\gamma = 1.06 \pm 0.34$ fm for their semi-theoretical model and $\gamma = 0.97 \pm 0.12$ fm for the phenomenological model of Meirav et al. [8].

Figure 2 shows results of global fits to 100 data points for pionic atoms, using the latest pion-nucleus potential with energy and density dependence in the s -wave term and finite range in the p -wave term, see [9] for details. The left hand side shows that the ‘skin’ shape for the neutron density distributions yields the lowest χ^2 value. The horizontal band represents the value of χ^2 per degree of freedom, which indicates the statistical significance of the fits and determines the uncertainty of the derived parameters, γ in this case. On the right hand side we compare data for Pb with predictions made with the global parameters of the left hand side. The results are consistent with the global analyses but the uncertainties are obviously considerably larger. This is typical also of antiprotonic atoms, demonstrating the limited accuracy of a single element analysis.

IV. DISCUSSION

Table I summarizes the above results regarding the shapes of the neutron density distributions, within the simple 2pF parameterization, and the values of the parameter γ of Eq.(2), which determines the dependence of the rms radius on the neutron excess parameter $(N - Z)/A$. The other parameter was held fixed at $\delta = -0.035$ fm. For antiprotonic atoms the two shapes of the neutron distributions lead to almost the same quality of fit and it is impossible to

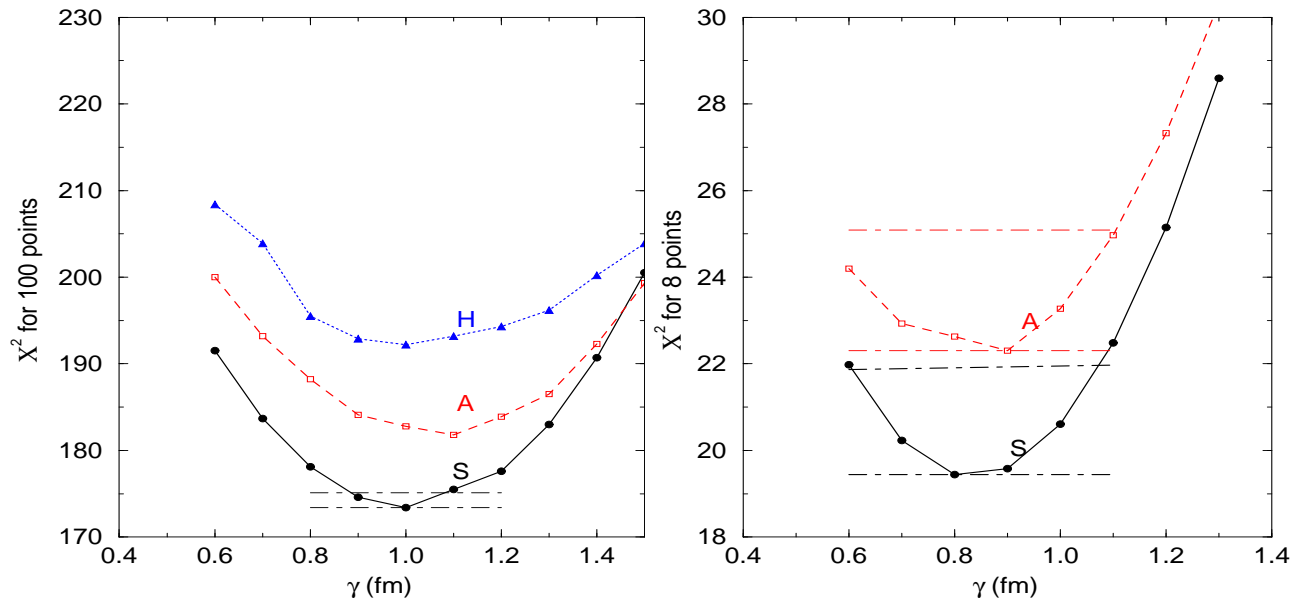


FIG. 2: Left: global fits to pionic atom data. S, A and H represent the skin, average and halo shapes, respectively. The horizontal band represents χ^2 per point, see text. Right: similar to the left but for pionic atoms of Pb.

TABLE I: Summary of results showing number of points and best fit values of χ^2 .

source	shape of ρ_n	N	χ^2	γ (fm)
\bar{p}	'halo'	90	196	0.9 ± 0.1
\bar{p}	'average'	90	198	1.25 ± 0.15
π^-	'skin'	100	173	1.0 ± 0.1

distinguish between the two on the basis of the values of χ^2 . The value of γ from pionic atoms is consistent with either values obtained from antiprotonic atoms but there seems to be a conflict considering the shape of the neutron density.

To look for the source of this conflict it is necessary to look into the radial sensitivities of the two probes, which have vastly different absorption cross sections in nuclear matter. This is done with the functional derivative method, introduced originally in connection with kaonic atoms [10] and later used also for pionic and antiprotonic atoms [9]. It is shown in [9] that pionic atom data are sensitive to nuclear densities around the 50% region of the central density whereas antiprotonic atom data depend on the density at the extreme periphery where the densities are well below 10% of the central density.

Figure 3 shows comparisons between the three versions of the 2pF neutron density and two, more physical, neutron densities for ^{208}Pb : (i) A single particle (SP) neutron density obtained by filling in of single particle levels in a common potential. (ii) A neutron density from a more sophisticated RMF calculation [11]. All five densities have the same rms radius. On the left hand side is indicated the sensitive region for pionic atoms and on the right hand side is indicated the sensitive region for antiprotonic atoms. It is evident that in the pionic atoms region the skin and the average shapes are closest to the SP and the RMF densities whereas in the antiprotonic atoms region the skin shape deviates markedly from the two more physical models. At very large radii the halo shape is very close to the RMF

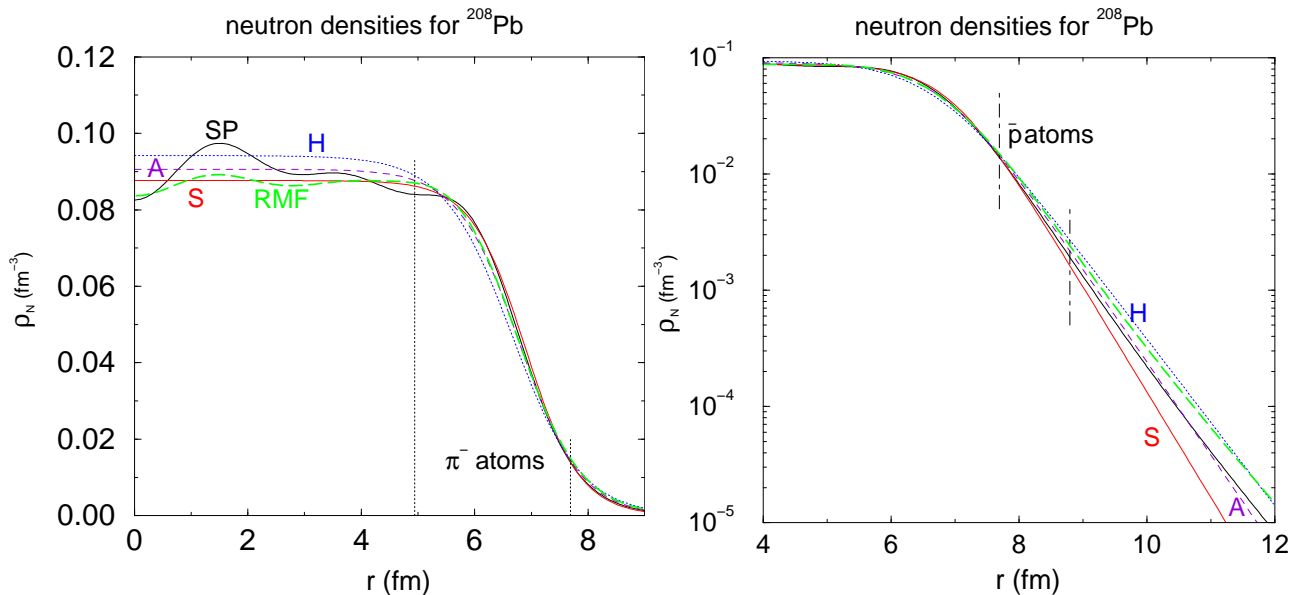


FIG. 3: SP and RMF neutron densities in ^{208}Pb compared with the three options of 2pF parameterizations (S for skin, H for halo and A for average). Left: covering the pionic atoms sensitive region. Right: covering the antiprotonic atoms sensitive region. All five densities have the same rms radius.

density but at the antiprotonic atoms region of sensitivity the average shape is equally good. The conclusion is that the 2pF model is not necessarily able to reproduce more realistic densities over a broad range of density values. In contrast it seems that the values of rms radii are less sensitive to the model used. We conclude that there is no real conflict between antiprotonic and pionic atoms and that on the average the rms radii of neutron density distributions in nuclei may be represented by Eq.(2) with $\gamma=1.0\pm 0.1$ fm and $\delta = -0.035$ fm. Applying this to ^{208}Pb which is a most studied nuclide, we find $r_n - r_p=0.18\pm 0.02$ fm, in very good agreement with Ref. [12].

Acknowledgments

I wish to thank A. Gal for many fruitful discussions and J. Mareš for providing some RMF densities.

-
- [1] C.J. Batty, E. Friedman, H.J. Gils, H. Rebel, Experimental methods for studying nuclear density distributions, *Adv. Nucl. Phys.* **19**, 1-188 (1989)
 - [2] J. Jastrzębski, A. Trzcińska, P. Lubiński, B. Klos, F.J. Hartmann, T. von Egidy, S. Wycech, Neutron density distributions from antiprotonic atoms compared with hadron scattering data, *Int. J. Mod. Phys. E* **13**, 343-351 (2004)
 - [3] A. Trzcińska, J. Jastrzębski, P. Lubiński, F.J. Hartmann, R. Schmidt, T. von Egidy, B. Klos, Neutron density distributions deduced from antiprotonic atoms, *Phys. Rev. Lett.* **87**, 082501-(1-4) (2001)
 - [4] E. Friedman, A. Gal, J. Mareš, Antiproton-nucleus potentials from global fits to antiprotonic X-rays and radiochemical data, *Nucl. Phys. A* **761**, 283-295 (2005)
 - [5] A. Trzcińska, J. Jastrzębski, T. Czosnyka, T. von Egidy, K. Gulda, F.J. Hartmann, J. Iwanicki, B. Ketzer, M. Kisieliński, B. Klos, W. Kurcewicz, P. Lubiński, P.J. Napiorkowski, L. Pieńkowski, R. Schmidt, E. Widmann, Information on antipro-

- tonic atoms and the nuclear periphery from the PS209 experiment, Nucl. Phys. A **692**, 176c-181c (2001)
- [6] C.J. Batty, E. Friedman, A. Gal, Density-dependent \bar{p} nucleus optical potentials from global fits to \bar{p} atom data, Nucl. Phys. A **592**, 487-512 (1995)
- [7] C. García-Recio, J. Nieves, E. Oset, Neutron distributions from pionic atoms, Nucl. Phys. A **547**, 473-487 (1992)
- [8] O. Meirav, E. Friedman, R.R. Johnson, R. Olszewski, P. Weber, Low energy pion-nucleus potentials from differential and integral data, Phys. Rev. C **40**, 843-849 (1989)
- [9] E. Friedman, A. Gal, In-medium nuclear interactions of low-energy hadrons, Phys. Rep. **452**, 89-153 (2007)
- [10] N. Barnea, E. Friedman, Radial sensitivity of kaonic atoms and strongly bound \bar{K} states, Phys. Rev. C **75**, 022202-(1-4)(R) (2007)
- [11] C.J. Horowitz, B.D. Serot, Self-consistent hartree description of finite nuclei in a relativistic quantum field theory, Nucl. Phys. A **368**, 503 (1981)
- [12] B. Kłos, A. Trzcińska, J. Jastrzębski, T. Czosnyka, M. Kisieliński, P. Lubiński, P. Napiorkowski, L. Pieńkowski, F.J. Hartmann, B. Ketzer, P. Ring, R. Schmidt, T. von Egidy, R. Smolańczuk, S. Wycech, K. Gulda, W. Kurcewicz, E. Widmann, Neutron density distributions from antiprotonic ^{208}Pb and ^{209}Bi atoms, Phys. Rev. C **76**, 014311-(1-13) (2007)